IOP Publishing Metrologia
Metrologia **57** (2020) 065003 (10pp) https://doi.org/10.1088/1681-7575/ab9ad4

Measuring atom positions in a microwave cavity to evaluate distributed cavity phase shifts

K Burrows[1], R J Hendricks[1], K Szymaniec[1], K Gibble[2], S Beattie[3] and B Jian[3]

[1] National Physical Laboratory, Hampton Road, Teddington TW11 0LW, United Kingdom
[2] Department of Physics, The Pennsylvania State University, University Park, PA 16802, United States of America
[3] National Research Council Canada, Ottawa, ON K1A 0R6, Canada

E-mail: krzysztof.szymaniec@npl.co.uk

Received 30 December 2019, revised 5 June 2020
Accepted for publication 9 June 2020
Published 15 October 2020

Abstract

Distributed cavity phase (DCP) frequency shifts are a leading systematic effect in atomic fountain frequency standards. They originate from the phase variations of the field in the microwave cavity combined with different positions of the atoms in the cavity on the ascent and descent. Here we demonstrate techniques to precisely determine the position of the cloud of atoms in the microwave cavity, using either the approximately linear variation of the transverse components of the microwave field or the quadratic variation of the longitudinal microwave field amplitude in the cavity. We also show that shifting the initial position of the atoms gives a significantly higher sensitivity to DCP variations than the often-used tilting of fountains. A demonstrated centring precision of order 50 μm will enable DCP frequency shift uncertainties to be reduced to less than 10^{-17} and thereby contribute insignificantly to the accuracy budget of a standard. These techniques to vertically align a fountain are straightforward to automate for routine operation and require a negligible fraction of the standard's averaging time.

Keywords: atomic clocks, frequency metrology, distributed cavity phase

(Some figures may appear in colour only in the online journal)

1. Introduction

Atomic fountain clocks provide the most accurate realization of the SI second definition and are operated by a growing number of national measurement institutes and other timing laboratories [1–6]. The existing designs and physical realizations are now relatively mature, and consequently the operation of fountains is robust [7]. If used as primary or secondary frequency standards, however, their full accuracy evaluation nonetheless requires significant time and effort. In particular, the distributed cavity phase (DCP) frequency shift is one of the systematic effects that is the most time consuming to characterize; its uncertainty dominates the overall uncertainty budget of the most accurate fountains [8–10]. Here we show that precise *in situ* position measurements and control of the position of the atomic cloud when it traverses the clock's microwave interrogation cavity can significantly reduce the DCP uncertainty and the time required to evaluate it.

The DCP frequency shift occurs because the atoms pass through the cylindrical microwave interrogation cavity at different horizontal positions during their upward and downward passages, and hence are sensitive to a spatial variation of the phase of the microwave field. A residual phase distribution of the field is unavoidable in any real cavity, which has finite surface resistivity, such that power flows from the feeds to the cavity walls. The effect is now well understood and a verified model makes it possible to evaluate the frequency bias and its uncertainty [11, 12]. The model expresses the correction as an azimuthal series, where only the lowest terms (m = 0, 1, 2) are significant. These terms correspond, respectively, to azimuthally symmetric longitudinal phase gradients (m = 0),

dipolar (m = 1) and quadrupolar phase variations (m = 2) [11, 13]. To reduce the phase gradients the cavities are fed at two or four positions around the cavity's circumference, at the mid-plane of the cavity, or by two feeds equidistant from it; in several fountains, there are two pairs of opposing feeds along perpendicular axes [7, 14, 15]. The DCP shift is small if the cloud's trajectory is close to vertical and near the cavity axis. In addition, the field coupled by the opposing feeds should have the same phase and amplitude. Conversely, feeding power to a single feed exaggerates the DCP m = 1 frequency shift and tilting the fountain along the direction of the feeds has been used to vertically align the fountain [12]. Unfortunately, in fountains with only one pair of independent feeds, this technique provides sensitivity to only one direction and, in some cases, it cannot be used at all if the feeds are not independently coupled to the microwave source [16]. Moreover, even if applicable, this procedure solely to vertically align the fountain requires long averaging times, as long as weeks.

A key parameter in the model is the centring of the atoms that are ultimately detected, during their cavity crossings. Rapidly and precisely determining the crossing positions would therefore expedite the DCP evaluation and reduce its uncertainty. Here we demonstrate two methods that use the microwave field in the clock cavity and its symmetry to measure the position of the atoms. One method exploits the variation of the amplitude of the microwave field across the cavity aperture, observed through the transition probabilities of the atoms. The second uses the radial component of the microwave field that grows linearly from the cavity axis, extending the previous work of [17]. The rapid measurement of the cavity crossing positions also serves as a diagnostic tool for fountain alignment, which involves changing the initial atom position and launch angle and overall fountain tilt such that the atom ensemble passes through the centre of cavity, on both its upward and downward passages. To illustrate the potential of these methods in reducing the DCP uncertainty, we refer to measurements performed on NPL-CsF3 and NRC-FCs2. Formal full accuracy evaluations of these primary frequency standards will be the subjects of separate publications [18].

2. Improving DCP evaluations

Of the three azimuthal contributions, the DCP m = 0 term leads to a negligible frequency shift ($<10^{-17}$) and the uncertainty from longitudinal phase gradients is small [8, 12, 19]. In the following subsection we show that the m = 1 and m = 2 terms can be evaluated with comparably small uncertainties using precise determinations of the cavity crossing position. The techniques enabling such precise determinations are described in detail in section 3.

2.1. DCP m = 1 contribution

The m = 1 phase gradient naturally leads to the largest DCP shift and uncertainty [11, 12]. It is minimized by balancing the amplitude and phase of opposing microwave cavity feeds, and by aligning the fountain to ensure a centred and vertical trajectory of the detected atom cloud. In general, the balance is ultimately checked by intentionally displacing the cloud on the two cavity crossings, minimizing and then setting a limit on the change of the clock's frequency. A residual frequency bias for an operating fountain is given by the slope and uncertainty of the measured frequency dependence on the cloud displacement, as shown in figure 1(a). Here, we show that precise measurements of the crossing position of the cloud in the microwave clock cavity enable setting a DCP m = 1 uncertainty, at 1×10^{-17} or less, significantly less than the best previously reported determinations of 6.4×10^{-17} [9].

To bound the slope in figure 1(a), it has become standard in DCP evaluations [12, 19, 20] to intentionally displace the cloud by tilting the fountain, and to measure the frequency difference versus tilt for several microwave amplitudes, e.g. $n = (1,3,5)\ \pi/2$ pulses, as in figure 2(a). The operating point is defined as the crossing point of the three lines and, considering measurement uncertainties, the spread of their crossings is associated with the uncertainty of the alignment. In figure 2(b), we show the same as figure 2(a) for a cloud that has a non-zero initial offset from the fountain axis. This currently standard approach thus leads to not only a substantial ambiguity in figure 2(b) [21], but also an operating point that can have a significant systematic error, larger than the statistical uncertainty. The direct measurements of the cloud positions in the cavity shown in section 3 avoid this systematic error.

A low DCP m = 1 uncertainty can be set with an accurate fountain alignment and a stringent limit on the slope in figure 1(a). Intentionally displacing the cloud with an initial launch offset does not noticeably degrade the clock stability over a larger range of displacements in the cavity (solid curve in figure 3(a)) as opposed to displacing the cloud by tilting the entire fountain (red dashed curve). The decrease in stability occurs due to the atomic cloud being clipped by fountain apertures more when tilting the fountain. Figure 3(b) shows the number of atoms detected versus the DCP m = 1 shift for a single feed, and thereby the sensitivity to any feed imbalance. For fountain tilts, the displacement on the ascent is small and, on the descent, the cloud has expanded well beyond the size of the cavity aperture and therefore a significant displacement is only possible when many of the atoms are blocked.[4] A small cloud with an initial offset is not significantly clipped on the ascent and the clipping for the expanded cloud on the descent is essentially unchanged. The DCP shift and therefore the sensitivity to feed imbalances is given predominantly by the ascending cloud passing through the cavity with the initial offset.

Our procedure to initially balance the feeds uses the atoms as a probe. The amplitude of the fields in the two feeding waveguides is independently adjusted and balanced by comparing

[4] We note the clipping biases the displacement of the atoms detected from the ascending cloud in the opposite direction as the displacement of the descending cloud, which increases the DCP shift and the sensitivity to feed imbalances. Nonetheless, the sensitivity is less than that for an initial cloud offset. Further, simultaneously employing an initial offset and a tilt can give even larger sensitivity for the same number of detected atoms.

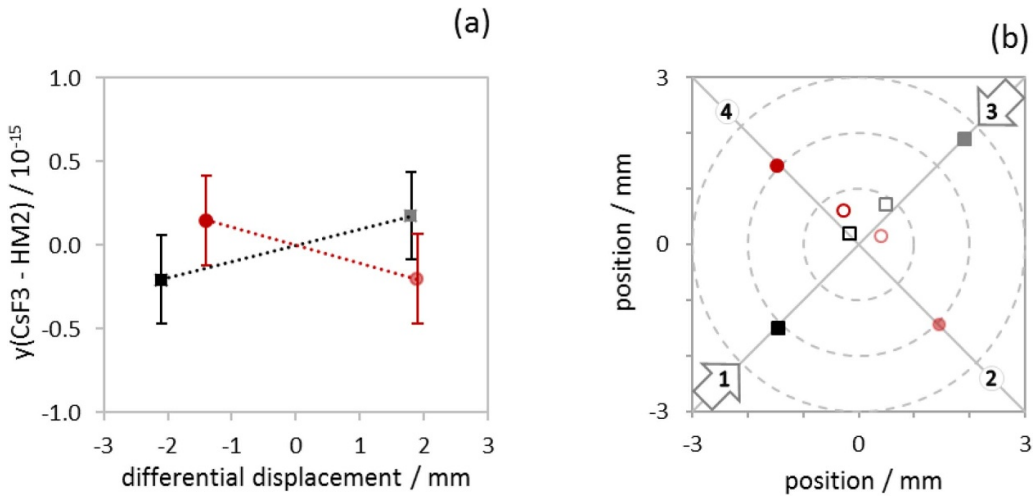

Figure 1. (a) Fractional frequency of the NPL-CsF3 fountain for balanced feeds as a function of the difference in displacement, between ascent and descent, of the detected atoms' mean position from the cavity centre, along (black squares) and orthogonal to (red circles) the feed axis. The four independent measurements were taken while alternating between displacements and the data points were corrected for an average frequency offset of the reference maser. Residual sensitivities to displacements along the two axes were inferred respectively as $(1.0 \pm 0.9) \times 10^{-16}$ mm^{-1} and $(-1.1 \pm 1.1) \times 10^{-16}$ mm^{-1}, which are consistent with zero within the measurement uncertainties. (b) Measured cavity crossing positions of the atom cloud on ascent (full symbols) and descent (open symbols) used to determine the DCP m = 1 frequency sensitivity; the large arrows indicate the feed axis. The correspondence of the data points in (a) and (b) is indicated with their shading.

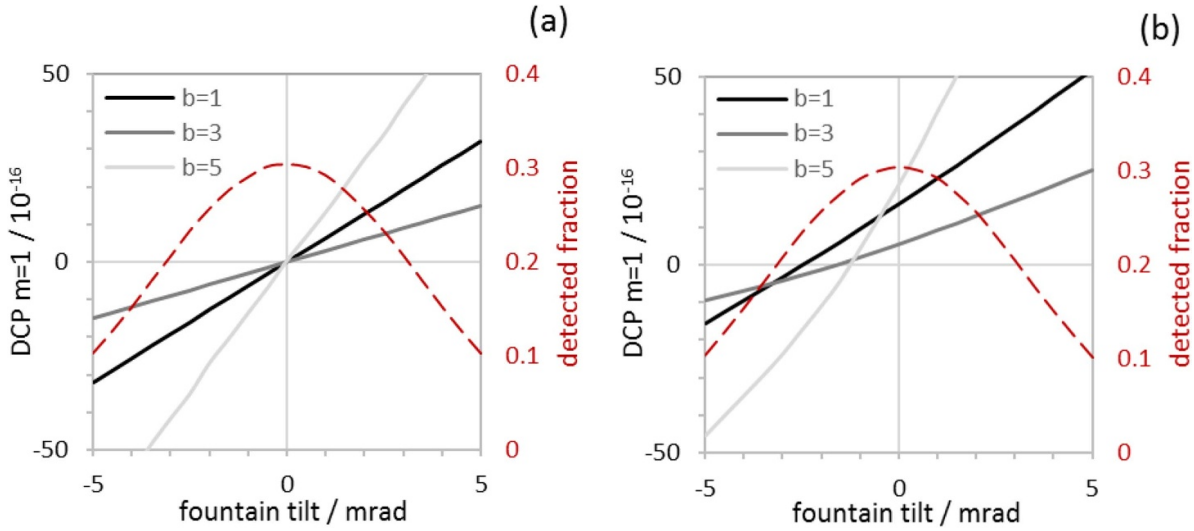

Figure 2. Calculated DCP m = 1 shifts versus fountain tilt for $b \times \pi/2$ pulses ($b = 1, 3, 5$) for (a) an initially centred cloud and (b) a cloud with a 2.5 mm initial offset and a launch angle that maximizes the number of detected atoms near zero tilt. In (a) the crossing of the $b = (1, 3, 5)$ DCP shifts accurately defines the operating point that has no sensitivity DCP m = 1 phase gradients for $\pi/2$ pulses, but there is not a single crossing in (b) and the crossing for $(b = 1, 3) \times \pi/2$ pulses can lead to a significant systematic tilt error. The dashed curves represent the fraction of atoms detected.

transition probabilities between the clock states when exciting the atoms using individual feeds; the phase is matched by optimising the transition probability for a single cavity passage when simultaneously feeding with two amplitude-balanced feeds. Reducing the phase imbalance below 10 mrad is sufficient to suppress the phase related contribution to DCP frequency shifts below 10^{-18} for the uncertainty of the detuning of the cavity's resonance in NPL-CsF2 [12, 19]. Balancing the field amplitudes to better than 1% would be sufficient to make the DCP m = 1 shift negligible, if both feeds were identical [9] and the surface resistivity around the cavity walls were uniform. In real cavities, however, unintended differences in the feeding waveguide cavities and potential patches in the resistivity (e.g. due to copper impurities or oxidation of the surface) could produce a significant phase gradient. The final check is therefore a measurement, as in figure 1(a).

To find the sensitivity to displacement of the DCP m = 1 frequency shift, we operate the fountain with one pair of balanced microwave feeds and shift the atom cloud crossing point

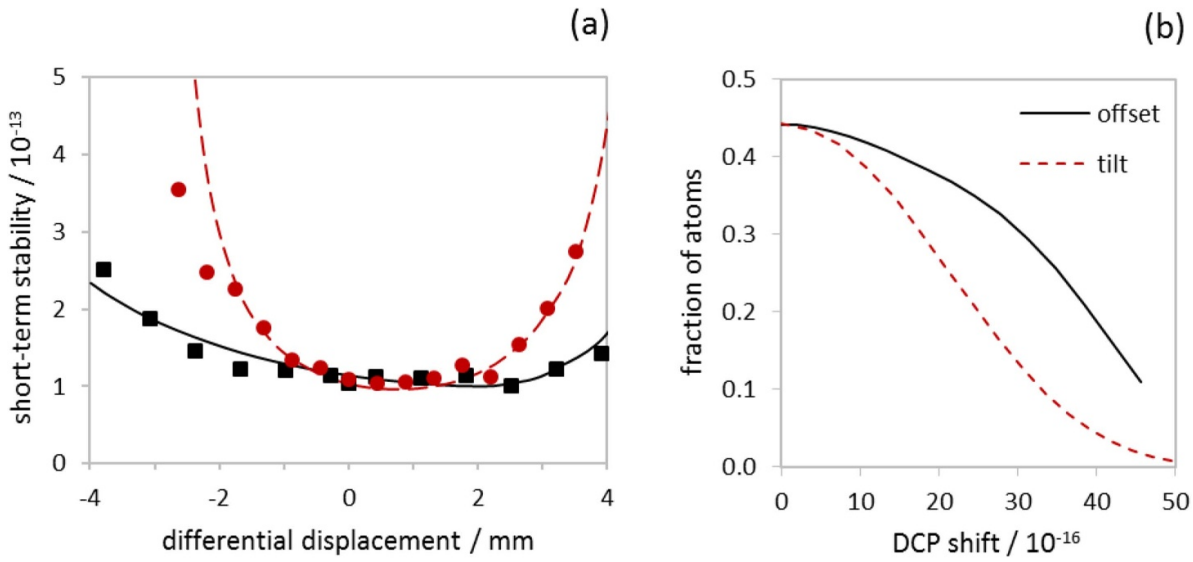

Figure 3. (a) Measured short-term stability (symbols) of NPL-CsF3 and simulation (curves) versus the difference of radial displacements of the cavity crossing points on the ascent and descent. The atom cloud was displaced by either tilting the fountain structure (red circles) or shifting the MOT position with shim coils (black squares). The asymmetry versus shift is due to a non-zero fountain tilt of 1.6 mrad. (b) Fraction of atoms detected versus DCP m = 1 shift for initial offsets (black solid curve) and fountain tilts (red dashed curve). Detecting more atoms using an initial offset yields a higher stability, and thereby a higher sensitivity to a residual feed imbalance, as in figure 1(a).

from the centre of the cavity along the feed axis. In fountains based on magneto-optical traps (MOT), the initial trap position and cavity crossing point of the cloud can be shifted by pulsing a set of shim coils around the cooling chamber shortly before the launch; we have used this technique and verified the cloud shift with a camera. Every 10 min we alternated between two positions of the MOT, as shown in figure 1(b), that correspond to displacements from the cavity centre for ascent (descent) of + 2.7 mm (0.9 mm) and −2.1 mm (0.0 mm) and an effective separation of 3.9 mm. The frequency measurement results after a total of 8 d of averaging are shown in figure 1(a). For displacements along the microwave feed axis, the frequency difference was $(3.8 \pm 3.7) \times 10^{-16}$. The error has both statistical and systematic contributions, where the latter is related to the collisional frequency shift and the DCP m = 2 shift (see below); the value of the frequency difference was corrected using the calculated m = 2 shift. Other systematic effects are common mode in this measurement. The results imply a DCP m = 1 frequency shift sensitivity slope, parallel to the microwave feed axis, of $(1.0 \pm 0.9) \times 10^{-16}$ mm^{-1}. Repeating the measurement using displacements perpendicular to the feed axis we obtain a frequency difference of $(-3.5 \pm 3.8) \times 10^{-16}$ for effective separations in the cavity of 3.3 mm, yielding a DCP m = 1 sensitivity to position along this axis of $(-1.1 \pm 1.1) \times 10^{-16}$ mm^{-1}.

As explained in section 3.2, our method for position determination enables verification of the alignment along the cavity axis for the detected part of the atom cloud to be centred, to less than 0.05 mm. Combining this with the measured DCP m = 1 sensitivities along the directions parallel and perpendicular to the microwave feed axis, including their uncertainties, we constrain the total DCP m = 1 frequency shift to be within $\pm 1 \times 10^{-17}$ (1σ), reducing this often-significant shift to be negligible.

2.2. *DCP m = 2 component*

Using the fine control and measurement of the cavity crossing points we have directly measured the DCP m = 2 frequency shift and found it to be consistent with the prediction for the NPL-CsF3 cavity. The fountain features two orthogonal pairs of microwave feeds so we measure the DCP m = 2 shift by alternately feeding with either pair of balanced opposing feeds and plot the frequency difference for several cloud positions (figure 4(b)). The DCP m = 2 shift scales quadratically with radial distance from the centre of the cavity and we again include cavity crossing positions that enhance the measurement sensitivity. Shim coils moved the initial MOT position such that cavity crossing positions on ascent were displaced by 2 mm from the axis in three azimuthal directions (figure 4(a)): along the two orthogonal feeding directions and symmetrically with respect to them (0° in figure 4(b)). For each displacement direction we alternated between the two pairs of balanced microwave feeds every 10 min. This reverses the sign of the DCP m = 2 frequency shift along a given feed pair axis, and hence the measured frequency difference for the two arrangements is equal to twice the corresponding m = 2 shift. For the symmetrical direction (0°) no frequency difference is expected. The field amplitudes coupled by the four feeds were balanced to better than 1%, individually and in pairs; the phase was matched for each pair of feeds. The measurement results are plotted in figure 4(b) along with a theoretical curve for the angular dependence of the m = 2 shift that treats the atomic trajectories [8–12, 15, 18]. The agreement with the model is good, within the measurement uncertainties, which are dominated by the statistical error after about 7 d of averaging at each position. A fit to the experimental data of DCP m = 2 shift taken at 2 mm from the cavity centre yields a peak value of $(1.1 \pm 0.8) \times 10^{-16}$, having corrected for the

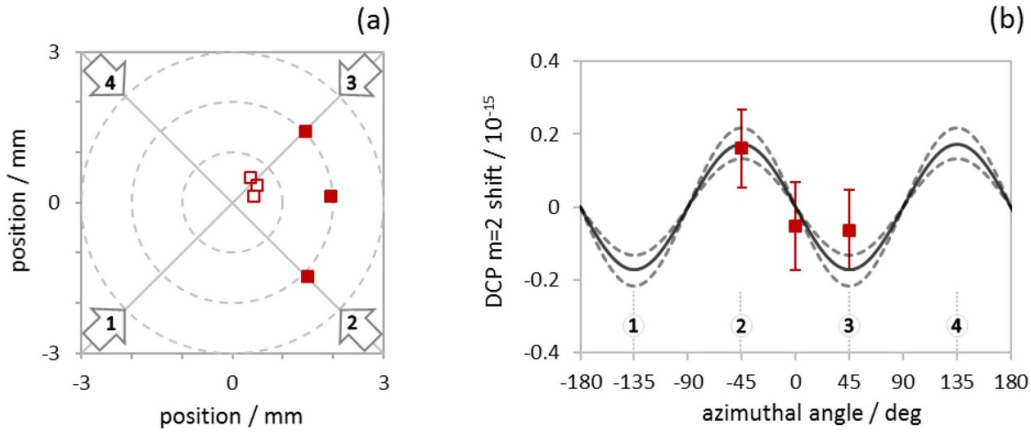

Figure 4. (a) Measured cavity crossing positions of the atom cloud on ascent (full symbols) and descent (open symbols) used to determine the DCP m = 2 frequency sensitivity; two pairs of balanced opposing feeds (large arrows) were used alternately. (b) Direct measurement (solid squares) and model predictions (curves) of DCP m = 2 frequency shift in NPL-CsF3. The measurements were taken for a 2 mm radial displacement in three azimuthal directions, as in (a), and the dotted lines with numbers show the feed orientations; the values plotted are obtained by subtracting the frequency measured using the orthogonal feeds (2 & 4) from the frequency obtained with the main feeds (1 & 3), and dividing the result by two. The dashed curves represent model bounds corresponding to 1-σ uncertainty from the crossing positions (see section 3.2).

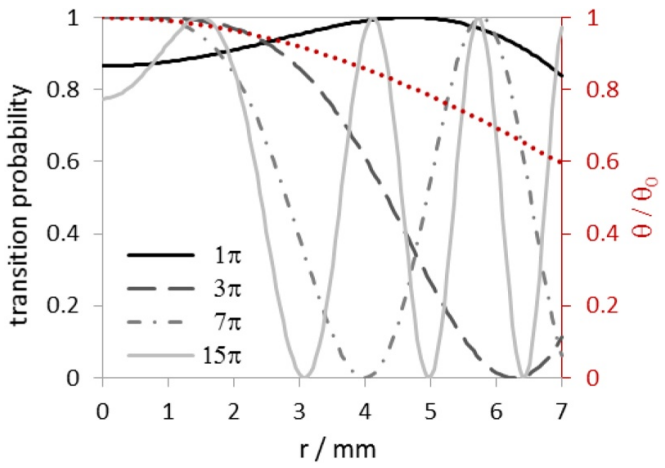

Figure 5. Transition probability versus transverse radial position in a microwave cavity for several pulse areas. The transverse variation of a 9.2 GHz microwave field in a cavity gives a variation of the tipping angle θ (dotted red curve) and in turn the variation of transition probabilities. Here, we note that the depicted pulse areas of 1 and 15π pulses are the usual average pulse area over the 7 mm cavity aperture, whereas the pulse areas for 3π and 7π are instead the peak pulse area on the cavity axis.

non-zero crossing point on descent. The corresponding theoretical peak value of the DCP m = 2 shift is 1.73×10^{-16}. For balanced feeds the residual m = 1 shift is at the level of 10^{-17} and it, as well as inhomogeneous density distributions and asymmetric wall losses,[5] can be neglected here. The measurements indicate that, for NPL-CsF3 and other fountains of similar design [7], the shift due to the centring of the atoms for normal operational parameters can be below 10^{-18} if the sub-ensemble of detected atoms is centred within 0.1 mm of the cavity axis on the ascent and descent, and remain < 10^{-17} if centred within 0.4 mm, for a cloud that is symmetric and has the same rms widths along the feed axes. We note also that for cavities with orthogonal pairs of opposing feeds, alternately or simultaneously using both pairs of feeds rigorously cancels their DCP m = 2 shifts.

[5] The DCP shift due to inhomogeneous wall losses (m = 0, 1, 2, …) does not contribute to this measurement.

3. Measurement of the cavity crossing positions

3.1. Rabi flopping method

Precisely determining the cavity crossing positions enables a more stringent DCP uncertainty as compared to earlier evaluations. One way to estimate the crossing positions relies on the microwave field amplitude variation across the cavity aperture. The amplitude peaks on axis and decreases approximately quadratically with increasing radius, as shown in figure 5 (red dotted curve). When shifting the MOT or tilting the fountain to displace the position at which the atoms cross the cavity, the transition probability (or equivalently the Rabi pulse area) changes in figure 6(a). Here, the microwave field is applied only on the ascent and the sensitivity is to the root-mean-square position of the detected atoms. As shown in figure 5, the sensitivity to the displacement from the cavity axis increases as the microwave amplitude increases—a π pulse has little spatial sensitivity and (3,5,7 …)π pulses have increasingly larger sensitivities close to the cavity axis. When launching small atomic clouds, the spatial sensitivity of the transition probability is largest around 13π; at higher microwave amplitudes the contrast of the Rabi oscillations decreases and reduces the sensitivity. Unfortunately, with an enhanced sensitivity to the change of the crossing position, the measurement is also more sensitive to the field amplitude instabilities. A way to circumvent this is to measure the change of the contrast of the Rabi flopping at a high amplitude, for example at 14π

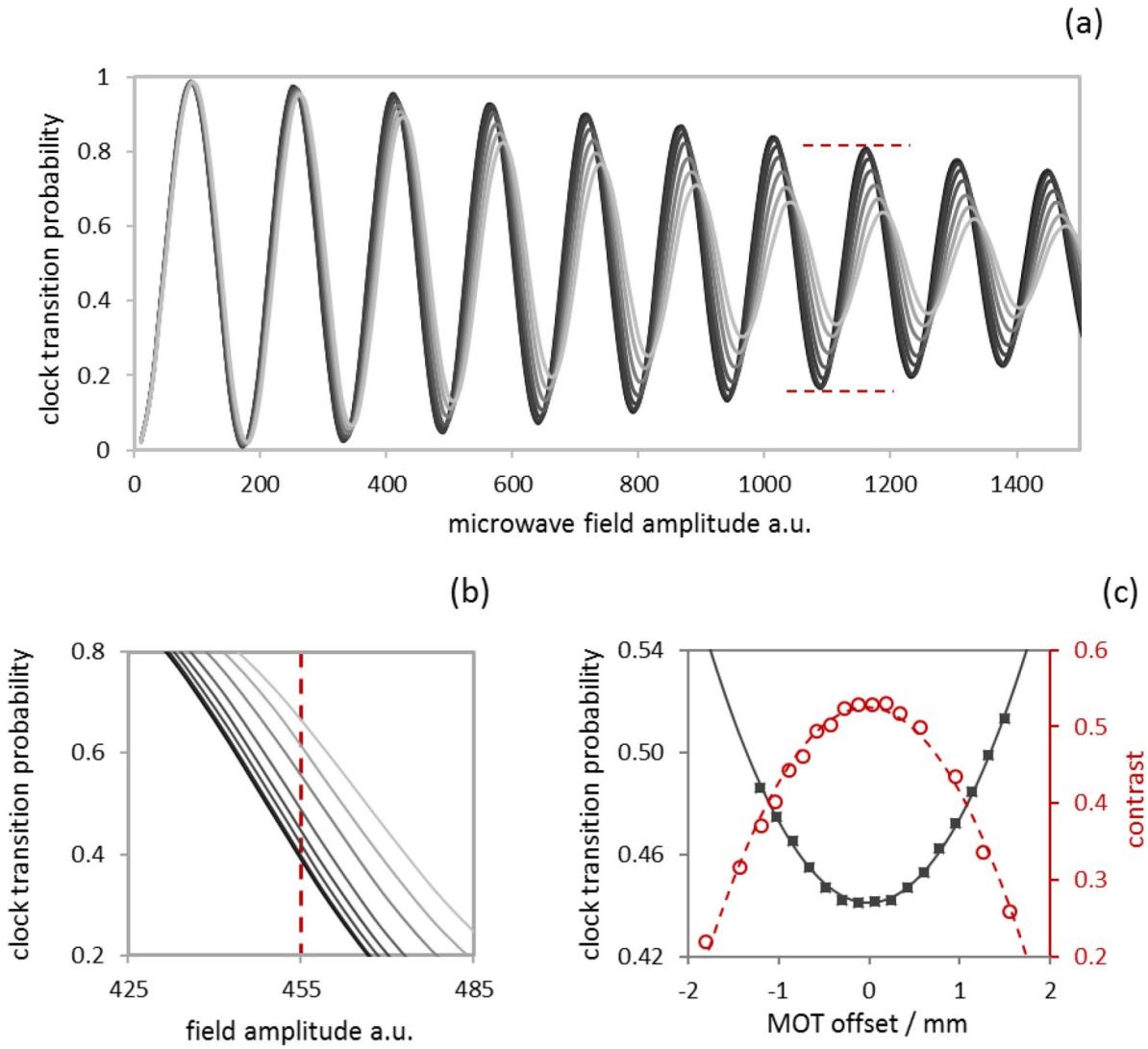

Figure 6. (a) Measured Rabi oscillations for several initial positions of the MOT; the microwave field was pulsed on only during the upward passage through the cavity. Lighter colours correspond to larger distances from the cavity centre, which result in a faster loss of contrast of the oscillations with the field amplitude. (b) An enlarged approximately linear section of the Rabi curve. (c) Clock transition probability measured for the field amplitude fixed near the position marked on (b) (black squares) and contrast of the Rabi flopping, as marked on (a) (red circles); the data are from NPL-CsF3 and NRC-FCs2, respectively. In both cases the data have parabolic dependences on the initial MOT positions and hence the corresponding cavity crossing position of the atoms.

and 15π (as marked in figure 6(a)), which gives our highest sensitivity.

The quadratic approximation of the field amplitude variation as well as the linear dependence of the cavity crossing point versus initial MOT position (or tilt) holds well for small (<5 mm) displacements from axis. In figure 6(c) we show an example of the change of the transition probability for an ascending cloud displaced in the cavity by moving the MOT. The MOT position (or equivalently the tilt) is centred for the upward cavity passage by operating at the mid-point of two values giving equal probability or contrast (figure 6(c)). We demonstrate a centring resolution of 0.3 mm.

The crossing position on the descent can be centred with a similar uncertainty if the fountain alignment also maximizes the amplitude of the time-of-flight detection signal [8]. However, this method is not accurate if the fountain's limiting aperture for the atoms is not at the cavity midplane[6] and the atoms are launched at a non-zero angle from the axis defined by the centres of the Ramsey cavity and the limiting aperture. In such case, the crossing position can be determined, and constraints placed on the DCP m = 1 shift, using a ballistic model of the expanding cloud in the fountain[7] [11]. Here, additional parameters for the model can be the fountain tilt of an extremum of the Rabi transition probability on the cloud's descent (for example at $5\pi/2$) [18]. The asymmetry of

[6] For example, in NPL-CsF3 and NRC-FCs2 the limiting aperture is 20.1 cm below the cavity midplane, near the end of a below cut-off waveguide.

[7] A cloud temperature of 2.0 μK was used in the model for NRC-FCs2 and NPL-CsF3. The corresponding cloud sizes (1/*e* radii) during cavity crossings were 3 mm for ascent and 11 mm for descent, clipped to 1.8 mm and 6.3 mm radii.

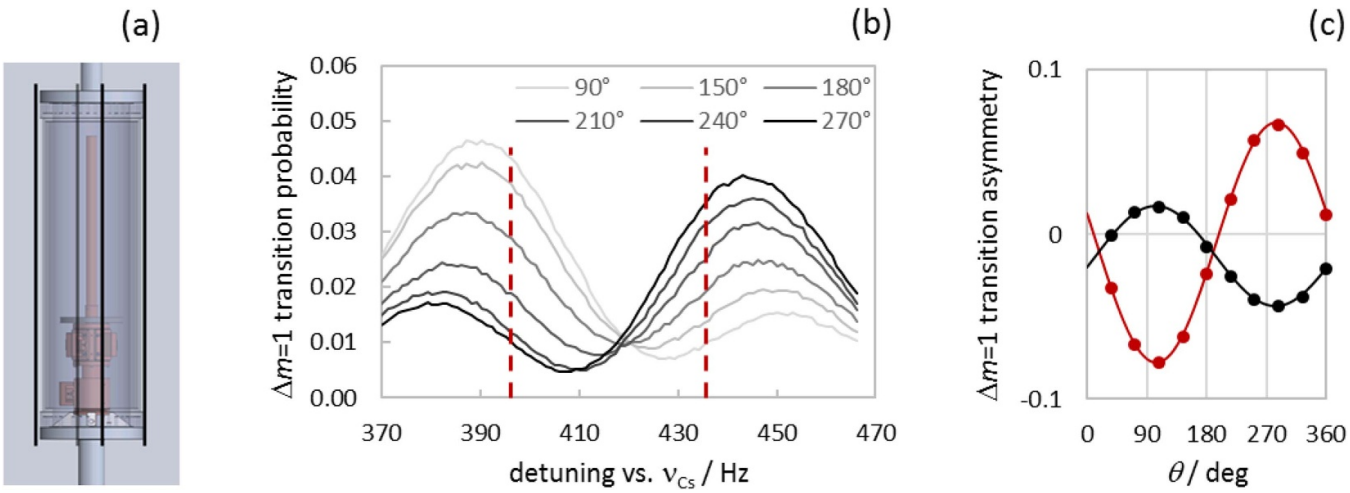

Figure 7. (a) Fountain schematic with four vertical conductors (black lines) to controllably tilt the C-field axis; the conductors are placed inside the magnetic shielding of the flight tube and carry currents of up to 1 mA. (b) Spectra of the suppressed $\Delta m = 1$ hyperfine transition for several orientations of the tilt of the C-field (see text); the microwave field amplitude was 10 times higher than during normal clock operation and turned on only for the ascent; the cloud was displaced 1.5 mm from the cavity axis. The resonant feature is symmetric (maximally asymmetric) for the C-field tilt parallel (perpendicular) to the cloud displacement. (c) Points: the asymmetries, i.e. the differences in transition probabilities measured for the detunings as marked in (b); curves: fitted sinusoids with amplitudes and phases corresponding to radial and azimuthal coordinates of the crossing position of the centre of the detected part of the atomic cloud. The two colours represent examples of different displacements (0.8 mm and 2.0 mm) with different azimuthal orientations. Angles are defined as in figure 4(b) and equation (1).

$\Delta m_F = 1$ transitions that we describe next offers higher resolution because it is linearly rather than quadratically sensitive to the positions of atoms in the cavity.

3.2. $\Delta m_f = 1$ transition asymmetry method

A second, potentially more precise, method to determine the cavity crossing positions *in situ* uses the small radial components of the TE_{011} standing wave. This method was first demonstrated by Nemitz *et al* [17] and exploits hyperfine σ transitions ($\Delta m_F = \pm 1$), which are inhibited by the fountain geometry when the oscillating magnetic field in the cavity is parallel to the static magnetic field, the C-field. The small transverse components are largest near the bottom and top cavity endcaps, with opposite directions so that atoms traversing the cavity away from the axis see a phase change of 180° of the radial field. The spectrum of these σ transitions is therefore a split doublet (see figure 7(b)) [17]. The probability of the σ transition increases if the C-field is tilted with respect to the cavity axis so that the main longitudinal oscillating field has a small component orthogonal to the C-field. The σ resonance doublets remain symmetric if the atoms cross the cavity on axis or are displaced from it along the transverse component of the tilted C-field. However, for atoms displaced perpendicular to the tilt plane, the horizontal components of the microwave field rotate (clockwise or counter-clockwise on either side of the cavity) and, as the corresponding parts of the doublet are enhanced, the shape becomes asymmetric (figure 7(b)). For small displacements of the cloud from the cavity axis, the asymmetry is linearly proportional to the displacement [17].

To fully utilize this technique, we have introduced a variable transverse magnetic field in our fountain, which creates an adjustable small angle between the C-field and the cavity axis in a controllable direction. Four vertical conductors were installed directly on the C-field solenoid at 90° intervals (figure 7(a)). By passing currents through the opposing pairs of wires connected in series, the transverse magnetic field can be varied in both magnitude and direction. Figure 7(b) shows the $\Delta m_F = 1$ doublets changing their shape as the transverse field is rotated by 360° with a constant magnitude with the same atom launch conditions. The largest asymmetry corresponds to a transverse field (and the C-field tilt plane) perpendicular to the atom cloud displacement from the cavity axis. The asymmetry $\Delta P_{\uparrow\downarrow}$ shown in figure 7(c) is simply the difference of the measured transition probability for two points equidistant in frequency, ± 20 Hz, from the $\Delta m_F = 1$ resonance (figure 7(b)) [17]. The resonance position can be obtained from a precisely measured Zeeman shift of a $\Delta m_F = 0$ field-sensitive transition. In figure 7(c), the measured asymmetry of the $\Delta m_F = 1$ doublet varies sinusoidally with the azimuthal angle of the added transverse magnetic field, θ; it can be expressed as:

$$\Delta P_{\uparrow\downarrow} \approx \pm[asin(\theta - -\phi_{\uparrow\downarrow}) + bsin(\theta_b - \phi_{\uparrow\downarrow})]r_{\uparrow\downarrow} \quad (1)$$

The amplitude of this sinusoid, the maximum change of the asymmetry, is proportional to the distance of the atoms from the cavity axis, $r_{\uparrow\downarrow}$, where the scaling constant a is determined through calibration with simulations. The phase $\phi_{\uparrow\downarrow}$ corresponds to the orientation of the passage position defined with respect to the installed set of wires, ± corresponds to ascent or descent, and the offset $bsin(\theta_b—\phi_{\uparrow\downarrow})$ results from a small constant residual transverse magnetic field at a fixed angle θ_b.

Figure 8(a) shows the positions in the cavity for the ascending cloud, which was changed by shifting the MOT and by

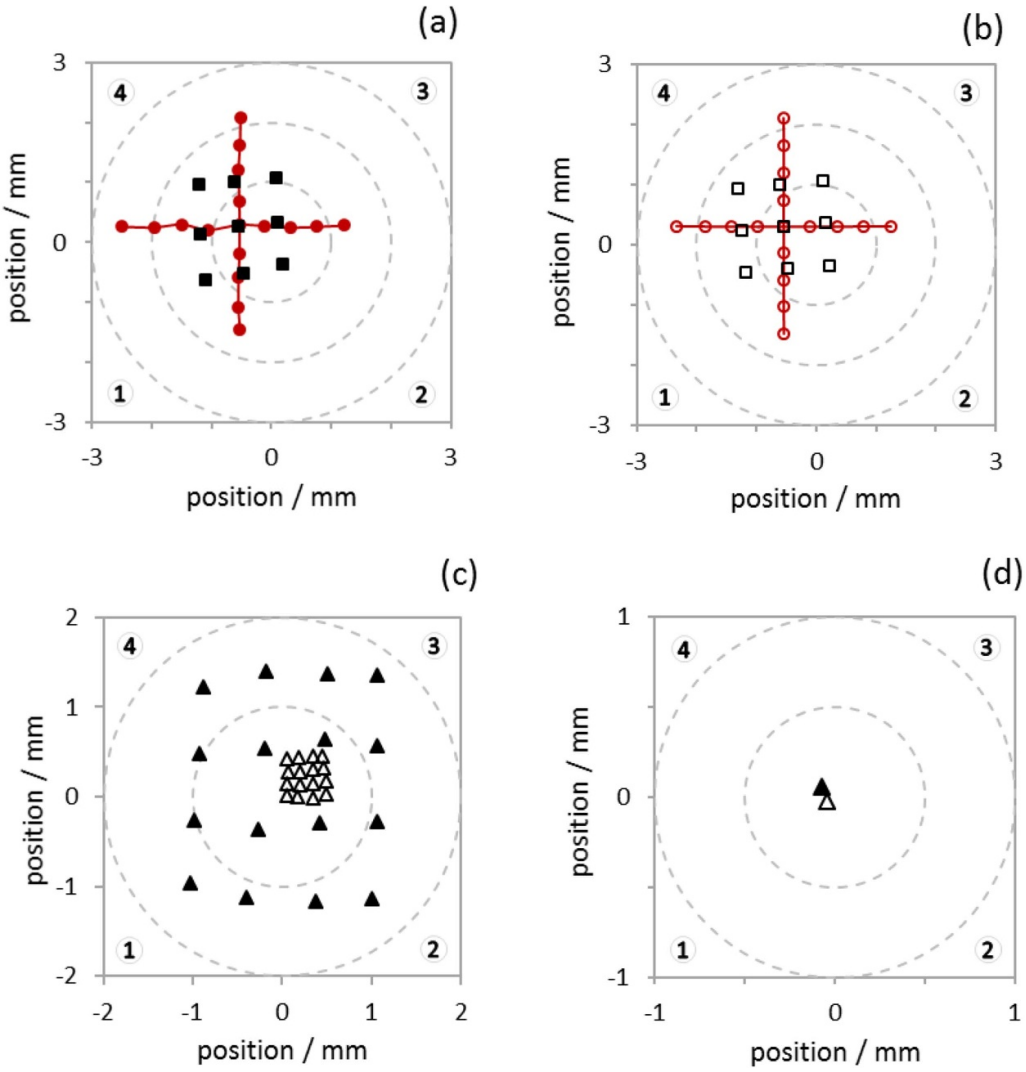

Figure 8. Measured (a) and simulated (b) cavity crossing positions on ascent for the centre of the detected sub-ensemble of the atomic cloud. The initial conditions at launch were varied by moving the MOT initial position (black squares, 0.9 mm step) or by tilting the entire fountain structure (red circles, 1.0 mrad step). The distances between the points in (a) were calibrated to match those in (b). (c) Corresponding crossing positions for ascent (full triangles) and descent (open triangles)—initial MOT position was moved on a grid with 0.9 mm step. In all cases the tilt of C-field was 3° from the cavity axis. (d) Positions after realignment (magnified); their relative distance and from the cavity centre is less than 50 μm. The numbers in corners of the plots are the same as in figures 1(b) and 4(a).

tilting the fountain structure. To relate the measured asymmetries to the actual positions in the cavity, we simulated the atomic trajectories for the cloud and fountain parameters and known changes of the initial position (MOT offset or tilt; figure 8(b)). The simulations are classical ballistic trajectories, ignoring atom-atom collisions. Trajectories crossing any modelled constraint in the physics package are rejected. For the remaining detected atoms, the mean horizontal position at the Ramsey cavity midplane was calculated for the upwards and downwards passages. Some of the cloud parameters were not known precisely *a priori* and their uncertainties were reduced by comparing the simulated changes in detected atom number and the relative crossing positions for ascent and descent with experimental observations. Finally, the calibration factors for the cavity displacement were established with a 16% uncertainty, which was dominated by our limited knowledge of the horizontal spread of atomic velocities. This uncertainty may affect the knowledge of crossing points at larger displacements (see figure 4 and DCP m = 2 measurement), but not when the fountain is reasonably well aligned. Here, the uncertainty of 0.06 mm is obtained after a single measurement due to a short-term noise of the resonance asymmetry measurement. After 15 min of averaging it decreases to 0.02 mm, limited mainly by the instability of launch direction and, consequently, the actual cavity crossing point (long term noise). We note as well that for the DCP m = 1 evaluation, the calibration of the displacements is not needed, only knowledge of the fractional deviation of the positions during normal operation with respect to the displacements used for the sensitivity measurements (figure 1).

To demonstrate the precision of the method, we measured the asymmetries and extracted the cloud positions, for both the ascending and descending cloud, as the MOT is moved over a grid of positions generated by the shim coils (figure 8(c)). As

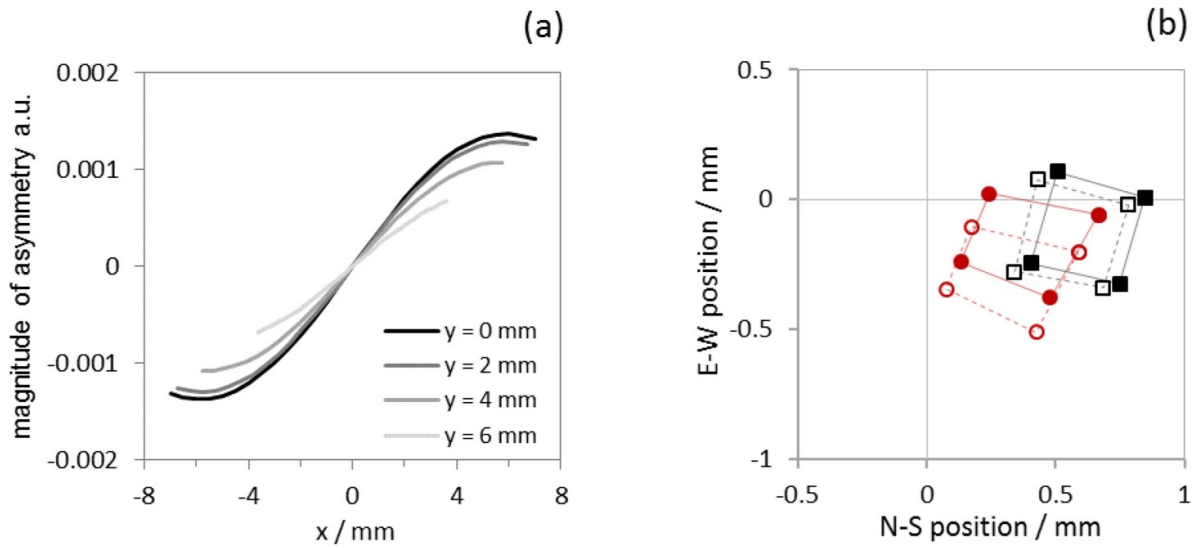

Figure 9. (a) Magnitude of the asymmetry of the $\Delta m_F = 1$ transition as a function of the atom's position. For atom offsets larger than 5 mm, the response becomes non-linear, even decreasing modestly beyond 6 mm. The linear sensitivity is also lower for atoms displaced along the transverse component of the C-field tilt, as shown for offsets of y = 2, 4, and 6 mm. (b) Cavity crossing positions on descent, measured separately for the radially inner (filled symbols) and outer (open symbols) parts of the cloud (see text). These are for two different alignments of the fountain and laser cooling beams (circles and squares); the initial cloud position was moved on an approximately 1 mm square. The perimeter of the resulting quadrilateral determines the radial scaling factor (i.e. $\Delta m_F = 1$ resonance asymmetry-to-position ratio). The crossing positions for the inner and outer parts of the cloud have average offsets of 140 μm and 70 μm for the two alignments. The residual scatter of the points (after compensating for the observed offset) is less than 20 μm.

expected, the measured displacements in the cavity are much smaller for the large descending cloud, but a grid pattern results nonetheless in figure 8(c). The sensitivity near the cavity axis for both ascent and descent makes this technique a useful tool to optimise the fountain tilt (figure 1(b)). In addition, the asymmetry measurement and fitting can be automated and the cavity crossing position can be determined in less than a minute of fountain operation.

The asymmetry of the $\Delta m_F = 1$ transition is approximately linear for small cloud displacements and then significantly deviates from linearity near the 7 mm radius of our cavity apertures, as shown in figure 9(a). This leads to a potential systematic error in the position measurements for the large atom cloud on the descent, if the centre of mass of the outer part of the cloud (atoms beyond 5 mm from the cavity axis where the displacement sensitivity decreases) is displaced from the centre of mass of atoms passing close to the axis. We use the field from our finite-element model of our precisely shaped interrogation cavity [14], including the endcap holes, which extends the treatment in [17]. On the ascent the cloud is small and the sensitivity is sufficiently linear. To check for this systematic error in determining the position of the descending cloud, we modified the sequence of pulses; after the $\Delta m_F = 1$ excitation in the Ramsey cavity ($|F = 4, m = 0\rangle \rightarrow |F = 3, m = 1\rangle$), an additional radiation pressure pulse clears the F = 4 population and a $\Delta m_F = 0$ microwave pulse selectively transfers only the central part of the cloud from $|3, 1\rangle$ to $|4, 1\rangle$ in the cylindrical selection cavity. This pulse is a 3π area pulse for atoms passing on the cavity axis (see figure 5) and transfers few atoms beyond 5 mm from the cavity axis. By measuring the asymmetry of the $\Delta m_F = 1$ resonance separately for the F = 3 (radially outer) and F = 4 (inner) groups of atoms, we probe potential differences in their average position; note that we probe atoms in both regions of the cavity on each fountain launch and see approximately equal fluorescence from each part. We have also confirmed the radial scaling factor for the inner and outer parts of the cloud by moving the initial MOT position and fitting the perimeter of the resulting quadrilateral (figure 9(b)). Initially we observed a 140 μm difference in the measured positions of the two parts of the cloud (figure 9(b)), suggesting that the non-linearity could be systematically shifting the measured average position of the entire cloud by about half this amount, or 70 μm. By changing the fountain and laser alignment we found that this systematic shift decreased to about 35 μm, and we expect that with further alignment it can reach the 20 μm limit from our launch direction instability.

4. Conclusions

We have demonstrated convenient techniques to precisely and rapidly establish cavity crossing positions for the detected atoms in a fountain clock. In contrast to previous DCP evaluations, finding the cavity crossing positions and aligning the fountain vertically does not rely on the orientation of the cavity feeds and the techniques can be implemented in fountains with cylindrical cavities of all designs and feeds arrangements. The implementation is straightforward and requires minimal or no modifications to a fountain. The simpler method of Rabi flopping, when aligning the fountain launch within the uncertainties used for the of NRC-FCs2 evaluation [18], can potentially constrain the DCP m = 1 frequency shift to below 3×10^{-17}. The upward crossing position in the

NPL-CsF3 cavity from this method agrees, within the combined uncertainties, with the more precise determination of the $\Delta m_F = 1$ transition asymmetry. This more precise method confirms the alignment of NPL-CsF3 with less than 50 μm separation of the detected atoms' mean position between the ascent and descent (figure 8(d)). After including the current instability of the launch direction (20 μm) and the above systematic uncertainty due to non-linearity (35 μm), the DCP m = 1 error is less than 1×10^{-17}. Here, we also find the predicted DCP m = 2 frequency shifts to be consistent with our experimental measurements and show that it can be controlled at a similar or lower level. In our approach, the only lengthy measurement is the frequency sensitivity to the displacement in the cavity for balanced feeds. Because the electrical properties of the cavity do not change rapidly, this measurement does not have to be repeated often. The more important potential drifts of the cloud position can be quickly and automatically checked and adjusted with these techniques.

Acknowledgments

We are grateful to Sang-Eon Park for stimulating conversations and Lewis Anderson for assistance in the NPL experiment; the NPL authors acknowledge financial support from the UK Department of Business, Energy and Industrial Strategy (as part of the National Measurement System program); and KG acknowledges financial support from the US National Science Foundation, grant 1607295 (Division of Physics).

ORCID iDs

K Burrows https://orcid.org/0000-0002-9795-4809
R J Hendricks https://orcid.org/0000-0002-5518-3719
K Szymaniec https://orcid.org/0000-0002-3523-278X
K Gibble https://orcid.org/0000-0003-3652-9638
S Beattie https://orcid.org/0000-0003-2056-2871
B Jian https://orcid.org/0000-0002-4588-3957

References

[1] Domnin Y S, Baryshev V N, Boyko A I, Elkin G A, Novoselov A V, Kopylov L N and Kupalov D S 2012 The MTsR-F2 fountain-type cesium frequency standard *Meas. Tech.* **55** 1155–62
[2] Fang F, Li M, Lin P, Chen W, Liu N, Lin Y, Wang P, Liu K, Suo R and Li T 2015 NIM5 Cs fountain clock and its evaluation *Metrologia* **52** 454–68
[3] Acharya A, Bharath V, Arora P, Yadav S, Agarwal A and Gupta A S 2017 Systematic uncertainty evaluation of the cesium fountain primary frequency standard at NPL India *MAPAN* **32** 67–76
[4] Dunst P, Nagorny B, Lemanski D, Nogas P, Nawrocki J, Hendricks R J, Ozimek F and Szymaniec K 2017 Preliminary evaluation of the AOS-CsF1 primary frequency standard *Proc. 31st Eur. Freq. and Time Forum* 628
[5] Beattie S, Alcock J, Jian B, Gertsvolf M and Bernard J 2016 Status of the atomic fountain clock at the National Research Council of Canada *J. Phys. Conf. Series* **723** 012008
[6] Jallageas A, Devenoges L, Petersen M, Morel J, Bernier L G, Schenker D, Thomann P and Südmeyer T 2018 First uncertainty evaluation of the FoCS-2 primary frequency standard *Metrologia* **55** 366–85
[7] Hendricks R J, Ozimek F, Szymaniec K, Nagorny B, Dunst P, Nawrocki J, Beattie S, Jian B and Gibble K 2018 Cs fountain clocks for commercial realizations—an improved and robust design *IEEE Trans. UFFC* **66** 624–31
[8] Weyers S, Gerginov V, Kazda M, Rahm J, Lipphardt D G and Gibble K 2018 Advances in the accuracy, stability, and reliability of the PTB primary fountain clocks *Metrologia* **55** 798–805
[9] Guena J *et al* 2012 Progress in atomic fountains at LNE-SYRTE *IEEE Trans. UFFC* **59** 391–410
[10] Szymaniec K, Lea S N, Gibble K, S-e P, Liu K and Glowacki P 2016 NPL Cs fountain frequency standards and the quest for the ultimate accuracy *J. Phys.: Conf. Ser.* **723** 012003
[11] Li R and Gibble K 2010 Evaluating and minimizing distributed cavity phase errors in atomic clocks *Metrologia* **47** 534–51
[12] Guena J, Li R, Gibble K, Bize S and Clairon A 2011 Evaluation of doppler shifts to improve the accuracy of primary atomic fountain clocks *Phys. Rev. Lett.* **106** 130801
[13] Li R and Gibble K 2004 Phase variations in microwave cavities for atomic clocks *Metrologia* **41** 376
[14] Gibble K, Lea S N and Szymaniec K 2012 A microwave cavity designed to minimize distributed cavity phase errors in a primary cesium frequency standard *Proc. Conf. Precis. Electromagn. Meas.* 700–1
[15] Park S E, Heo M-S, Kwon T Y, Gibble K, Lee S-B, Park C Y, Lee W-K and Yu D-H 2014 Accuracy evaluation of the KRISS-F1 fountain clock *Proc. IEEE Int. Freq. Control Symp*. (https://doi.org/10.1109/FCS.2014.6859971)
[16] Weyers S, Gerginov V, Nemitz N, Li R and Gibble K 2012 Distributed cavity phase frequency shifts of the caesium fountain PTB-CSF2 *Metrologia* **49** 82–87
[17] Nemitz N, Gerginov V, Wynands R and Weyers S 2012 Atomic trajectory characterization in a fountain clock based on the spectrum of a hyperfine transition *Metrologia* **49** 468–78
[18] Beattie S, Jian B, Alcock A J, Gertsvolf M, Hendricks R J, Szymaniec K and Gibble K 2020 First accuracy evaluation of the NRC-FCs2 primary frequency standard *Metrologia* **57** 035010
[19] Li R, Gibble K and Szymaniec K 2011 Improved accuracy of the NPL-CsF2 primary frequency standard: evaluation of distributed cavity phase and microwave lensing frequency shifts *Metrologia* **48** 283–9
[20] Chapelet F, Bize S, Wolf P, Santarelli G, Rosenbusch P, Tobar M E, Laurent P, Salomon C and Clairon A 2006 Investigation of the distributed cavity phase shift in an atomic fountain *Proc. 20th Eur. Freq. and Time Forum* (https://www.eftf.org/fileadmin/conferences/eftf/documents/Proceedings/proceedingsEFTF2006.pdf)
[21] Lee S, Heo M-S, Kwon T Y, Hong H-G, Lee S-B and Park S E 2018 An alignment technique for optimal atomic trajectory of an atomic fountain clock *32nd Eur. Freq. and Time Forum*